View metadata, citation and similar papers at core.ac.uk

brought to you by CORE

provided by Open Access LMU

Materials Chemistry

Cite this: *J. Mater. Chem.*, 2011, **21**, 13817

www.rsc.org/materials

PAPER

All-inorganic core–shell silica–titania mesoporous colloidal nanoparticles showing orthogonal functionality†

Valentina Cauda,[ab] Johann M. Szeifert,[a] Karin Merk,[a] Dina Fattakhova-Rohlfing[a] and Thomas Bein*[a]

Received 25th December 2010, Accepted 16th May 2011
DOI: 10.1039/c0jm04528d

Downloaded by Ludwig Maximilians Universitaet Muenchen on 25/04/2013 13:29:51.
Published on 10 August 2011 on http://pubs.rsc.org | doi:10.1039/C0JM04528D

Colloidal mesoporous silica (CMS) nanoparticles with a thin titania-enriched outer shell showing a spatially resolved functionality were synthesized by a delayed co-condensation approach. The titania-shell can serve as a selective nucleation site for the growth of nanocrystalline anatase clusters. These fully inorganic pure silica-core titania-enriched shell mesoporous nanoparticles show orthogonal functionality, demonstrated through the selective adsorption of a carboxylate-containing ruthenium N3-dye. UV-Vis and fluorescence spectroscopy indicate the strong interaction of the N3-dye with the titania-phase at the outer shell of the CMS nanoparticles. In particular, this interaction and thus the selective functionalization are greatly enhanced when anatase nanocrystallites are nucleated at the titania-enriched shell surface.

Introduction

Colloidal mesoporous silica (CMS) nanoparticles are of great interest as potential candidates for applications in gas-sensing,[1] host–guest chemistry and drug delivery.[2,3] The functionality of the CMS is caused by their large surface area and a mesoporous structure with tunable pore size, which makes them ideal hosts for the accommodation of various guest species. Most of the intended applications require silica nanoparticles with specific organic or inorganic functionalization, thus providing properties not obtainable from pure silica materials.[4] A special advantage of mesoporous silica nanoparticles is their chemical versatility and solution processability, making it possible to selectively functionalize different locations on the nanoparticle, for example inner pore volume and outer particle surface.[5,6] By using different functional groups, even nanoparticles with site-specific orthogonal functionality can be obtained.[7] In most cases, however, this extended functionality comes at the cost of limited thermal or chemical stability.

We propose the combination of two metal oxides such as silica and titania as an alternative approach toward the generation of core–shell nanoparticles with orthogonal chemical functionality. Titanium dioxide is commonly used as an inexpensive, non-toxic pigment. Additionally, its semiconducting properties are used in applications including non-silicon solar cells, photocatalysis and energy storage, respectively.[8] Although both silica and titania are chemically related and form solid solutions, titania exhibits different functionality and chemical reactivity. In contrast to silica, the titania surface shows a higher stability in basic media and has a strong affinity to acidic groups such as carboxylic or phosphonic acids, which is often used for the grafting of acid-containing moieties.[9] Previous examples of the spatially resolved combination of both materials in a single nanoparticle are related to the deposition of a thin titania shell on non-porous silica nanoparticles,[10,11] thus obtaining a good spatial definition of titania in highly dispersed colloids. Recently, silica–titania hollow nanoparticles were fabricated to study the cellular uptake and cytotoxicity in living cancer cells for drug delivery applications.[12] Other combinations of silica and titania in the form of thin films or bulk materials have been investigated with a view on different applications, including photocatalysis,[13,14] catalysis,[15] and optical devices[16–18] for chemical sensing.

Mesoporous titania–silica composites are primarily synthesized following two synthetic strategies. The first approach is the mixing of the two sol–gel precursors, or silica sol–gel and titania nanoparticles and subsequent surfactant-assisted assembly into a mesoporous structure.[13–15,19] This procedure is useful for obtaining well-ordered structures, especially in thin films, however, no spatially selective functionalization can be achieved. The second pathway involves the templated self-assembly of bulk mesoporous silica followed by post-modification using a titania precursor, resulting in a mostly amorphous TiO_2 shell.[20,21] These composite materials feature the chemical reactivity of titania coupled with a high surface area and good thermal stability. However, the post-synthetic coating of the bulk mesoporous silica often covers the pore openings, resulting in limited accessible pore volume. Furthermore, control over the spatial

[a]*Department of Chemistry and Center for NanoScience (CeNS), University of Munich, Butenandtstrasse 11, 81377 Munich, Germany. E-mail: bein@lmu.de; Fax: +49 (0)89 2180 77622; Tel: +49 (0)89 2180 77623*

[b]*CSHR@Polito, Italian Institute of Technology (IIT), C. so Trento 21, 10129 Turin, Italy*

† Electronic supporting information available: ζ-Potential data of the different samples are available free of charge. See DOI: 10.1039/c0jm04528d

Downloaded by Ludwig Maximilians Universitaet Muenchen on 25/04/2013 13:29:51.
Published on 10 August 2011 on http://pubs.rsc.org | doi:10.1039/C0JM04528D

distribution of the two oxides is not possible in this case. The above-mentioned synthetic methods commonly rely on a final calcination step to achieve crystallization of titania. Such a calcination step would preclude the synthesis of colloidal systems due to irreversible agglomeration and loss of dispersibility.

Here we report the low-temperature preparation of colloidal mesoporous silica-core/titania-enriched shell nanoparticles with spatially resolved functionality. Instead of incorporating Ti atoms throughout the whole CMS nanoparticle, titania is selectively introduced at the outer shell of the mesoporous silica nanoparticles by a delayed co-condensation approach, in analogy to the site-selective functionalization previously reported by us[5,6] (Scheme 1).

Different Si/Ti ratios in the nanoparticle shells were obtained by changing the titania precursor stoichiometry. Furthermore, crystalline titania shells were also obtained *via* nucleation of anatase on the amorphous titania shell from a benzyl alcohol reaction system.[22,23] This non-aqueous approach avoids the use of high temperature treatments, which would lead to irreversible particle aggregation. As a proof of principle addressing the spatially selective reactivity we demonstrate, with optical spectroscopy, the selective adsorption of the carboxylate-containing ruthenium dye N3[24,25] and its fluorescence quenching upon specific adsorption to the titania sites.

Key features of these titania-enriched shell mesoporous silica nanoparticles include their spatially resolved, thus "chemically orthogonal" functionality, the biocompatibility of the two inorganic oxides, and their high porosity and nanoscopic size. These features can be attractive for drug delivery applications, bioimaging and diagnostics. In addition, the titania-containing shell is expected to protect the mesoporous silica core against degradation by biological fluids due to its higher chemical stability.

Materials and methods

Synthesis of the mesoporous nanoparticles

The pure silica CMS nanoparticles (sample CMS) were synthesized according to a procedure described elsewhere.[4] Briefly, 1.92 g tetraethylorthosilicate (TEOS; 9.22 mmol; Fluka, >98%) and 14.3 g triethanolamine (TEA; 95.6 mmol; Aldrich, 98%) were heated at 90 °C for 20 min without stirring in a polypropylene reactor (sol. 1). Thereafter, a second solution (sol. 2) of 2.41 mL cetyltrimethylammonium chloride (CTAC; 1.93 mmol; Fluka, 25% in H_2O) and 21.7 g (1.21 mol) bi-distilled water from a Millipore system (Milli-Q Academic A10) was prepared. It was heated at 60 °C for 20 min and then added to the sol. 1. The resulting mixture with a molar ratio of 1.0 TEOS : 0.2 CTAC : 10.37 TEA : 130.15H_2O was stirred at 500 rpm RT overnight. The nanoparticles were then isolated by centrifugation (19 000 rpm, 43 146 RCF, 20 min) and re-suspended in absolute ethanol.

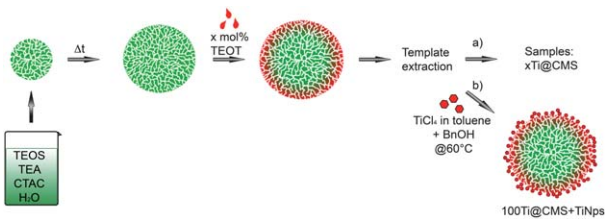

Scheme 1 Synthetic pathway for the titania-shell colloidal mesoporous silica (CMS) nanoparticles. A delayed co-condensation approach is used to first synthesize the mesoporous silica core (in green) and then enrich the outer surface (in red) with the titania-phase, followed by template extraction. (a) Depending on the molar amount of TEOT added (with respect to the initial amount of silica) different *x*Ti@CMS samples are obtained. (b) The sample with the highest amount of Ti, 100Ti@CMS (see Table 1), was used to nucleate anatase nanocrystallites (TiNPs) on the outer shell, increasing the orthogonality of the system (abbreviations: see Materials and Methods).

The titania-enriched shell nanoparticles were synthesized by a procedure similar to our previously developed delayed co-condensation approach.[5,6] After combining sol. 1 and sol. 2, the mixture was stirred at 500 rpm for 20 minutes. Then a certain amount *x* of tetraethyl orthotitanate (TEOT, Aldrich, >98%) was divided into 20 portions and added at 30 second intervals giving a total molar ratio TEOT/TEOS of 0.1; 0.5; 0.8; 1.0, respectively (sample codes *x*Ti@CMS, see Table 1). The mixture was then stirred at 500 rpm at room temperature overnight. The template was extracted by heating the samples in a solution of 2.0 g (25.0 mmol) ammonium nitrate in 100 mL absolute ethanol for 45 min under reflux. After centrifugation (19 000 rpm, 43 146 RCF, 30 min) and re-suspending in absolute ethanol, a second extraction step with 10 mL of concentrated hydrochloric acid and 90 mL of absolute ethanol was carried out under reflux for 45 min. Afterwards, the colloidal mesoporous nanoparticles were again separated by centrifugation and redispersed in absolute EtOH.

To determine the concentration of nanoparticles, a known volume of colloidal solution was dried at 60 °C and the residue weighed.

The sample 100Ti@CMS was further used as a starting material for the growth of titania nanocrystallites at the outer surface of the mesoporous nanoparticles.[22] For this purpose, a solution of titanium tetrachloride (Aldrich, 1.0 mL, 9.22 mmol) in toluene (6.7 mL, at a ratio $TiCl_4$: toluene = 1 : 0.15) was added to water-free benzyl alcohol (Aldrich, 13.3 mL, 139.4 mmol, at a ratio BnOH : toluene = 3 : 2) under continuous stirring and then poured into the template-extracted 100Ti@CMS colloidal suspension (9.22 mmol of the silica content) in absolute EtOH under continuous stirring. The mixture was kept at 60 °C overnight to induce the formation of crystalline TiO_2 nanoparticles (thus the sample name 100Ti@CMS + TiNPs) and afterwards washed twice with abs. EtOH by centrifugation (19 000 rpm, 43 146 RCF, 20 min). All the samples were washed with bi-distilled water for 2 h and redispersed in absolute EtOH before characterization. The dried sample 100Ti@CMS + TiNPs was also calcined at 450 °C for 4 h (at a ramp of 1 °C min^{-1}) in air.

Characterization techniques

Dynamic light scattering (DLS) and ζ-potential measurements were carried out with a Malvern Zetasizer-Nano instrument with a 4 mW He–Ne laser (λ = 633 nm) and an avalanche photodetector. DLS measurements were performed on diluted ethanolic suspensions (at a conc. of 1 mg mL^{-1}), whereas for the

 This journal is © The Royal Society of Chemistry 2011

Table 1 List of samples with molar ratio and molar amount of TEOT added in the synthetic mixture and their structural parameters

Sample	Molar ratio[a] TEOT/TEOS	Total amount of TEOT/mmol	BET surface area/m^2 g^{-1}	Pore size/nm	Pore volume/cm^3 g^{-1}
CMS	0	0	1056	3.8	0.89
10Ti@CMS	0.1	0.92	1009	3.8	0.77
50Ti@CMS	0.5	4.61	1187	3.7	0.88
80Ti@CMS	0.8	7.38	963	3.8	0.72
100Ti@CMS	1	9.22	1115	3.7	0.87
100Ti@CMS+ TiNPs	1 + 1 TiNPs[b]	9.22 + $TiCl_4$	1279	4.2	1.15

[a] Total molar ratio of TEOT added *vs.* initial amount of TEOS in the synthesis solution. [b] The quantity 1 TiNPs refers to a molar ratio of 1 : 1 between $TiCl_4$ and the initial amount of TEOS.

Downloaded by Ludwig Maximilians Universitaet Muenchen on 25/04/2013 13:29:51.
Published on 10 August 2011 on http://pubs.rsc.org | doi:10.1039/C0JM04528D

determination of the ζ potential profiles, one drop of the ethanolic suspension (~3 wt%) was mixed prior to measurement with 2 mL commercial Hydrion Buffer solutions, having pH values of 2, 3, 4, 5 and 6, respectively. UV-Vis measurements were performed on a UV-Vis spectrophotometer (Hitachi U-3501) with ethanolic suspensions of the nanoparticles (conc. 1.15 mg mL^{-1}) in a 1 mm path length cuvette. X-Ray diffraction was carried out in reflection mode using a Bruker D8 Discover with Ni-filtered CuKα-radiation and a position-sensitive detector (Vantec). Nitrogen sorption measurements were performed on all samples with a Quantachrome Instruments NOVA 4000e at 77 K. Pore size distribution and volume were calculated with a NLDFT equilibrium model of N_2 on silica. The pore volume was determined up to a pore size of 8 nm in order to eliminate the contribution of interparticle textural mesoporosity. The specific surface area was estimated using a BET model. For Transmission Electron Microscopy (TEM) and Scanning Transmission Electron Microscopy (STEM) a Titan 80–300 microscope operating at 300 kV equipped with a high-angle annular dark field (HAADF) detector was used and a drop of the diluted colloidal suspension was dried on a carbon-coated copper grid. Fluorescence measurements were performed on a PTI spectrofluorometer with a photomultiplier detection system (model 810/814) and a xenon arc lamp. For all samples a 1 cm quartz cuvette with a volume of 3 mL was used.

N3-Dye adsorption

The amount of 5 mg of samples CMS, 100Ti@CMS and 100Ti@CMS + TiNPs, respectively was added to 500 μL of *cis*-bis(isothiocyanato)bis(2,2′-bipyridyl-4,4′-dicarboxylato) ruthenium(II) (99% Aldrich, N3 hereafter) in water (0.6 mM) and stirred in the dark for 1 hour. Then the particles were separated by centrifugation (20 000 rpm, 47 807 RCF, 15 min) and washed 3 times with bi-distilled water for 1 h each. Finally, the N3-loaded samples were dispersed in water at a conc. of 1.15 mg mL^{-1}. The UV-Vis spectra of the N3-solution before and after adsorption, and of the colloidal suspensions of N3-loaded samples were recorded. For the fluorescence measurements, 100 μL of N3-loaded nanoparticle suspension was diluted in 3 mL water (0.038 mg mL^{-1}).

Results and discussion

Mesoporous nanoparticle characterization

A solution of TEOS and triethanolamine (TEA) in water with the template, cetyltrimethylammonium chloride (CTAC), leads to the growth of CMS nanoparticles. After 20 min the titania source (TEOT) is added to the uncompleted CMS synthetic mixture, leading to a co-condensation of silica and titania precursors. We anticipate that the resulting colloidal nanoparticles consist of a mesoporous silica core and a titania-enriched mesoporous silica shell. By varying the added amount of TEOT, different Si/Ti ratios in the resulting nanoparticle shells were obtained. Furthermore, a precursor solution for the synthesis of crystalline titania nanoparticles (TiNPs) of about 4 nm in diameter in benzyl alcohol[22] is added to the titania-shell CMS nanoparticles having the highest content of titania.

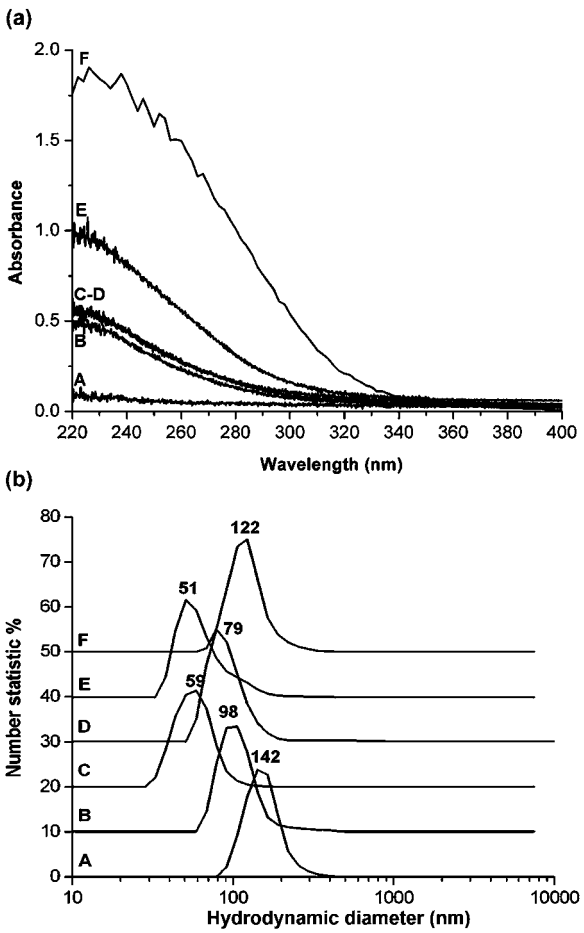

Fig. 1 (a) UV-Vis spectra and (b) dynamic light scattering data of the samples: A: CMS; B: 10Ti@CMS; C: 50Ti@CMS; D: 80Ti@CMS; E: 100Ti@CMS; F: 100Ti@CMS + TiNPs. For clarity, the DLS curves are shifted along the *y*-axis by 10 units each.

Downloaded by Ludwig Maximilians Universitaet Muenchen on 25/04/2013 13:29:51.
Published on 10 August 2011 on http://pubs.rsc.org | doi:10.1039/C0JM04528D

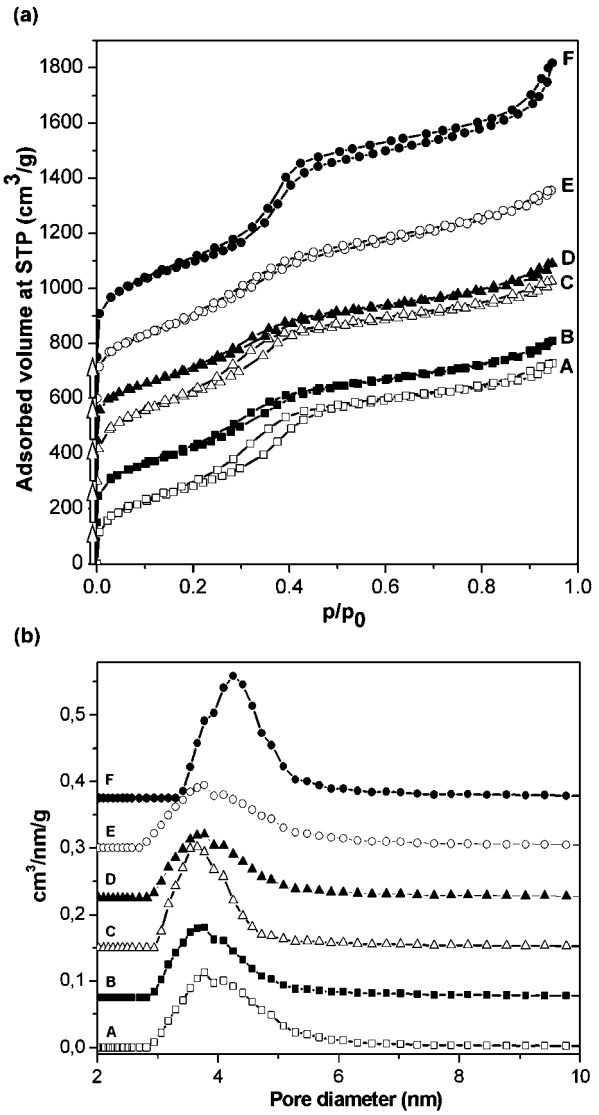

Fig. 2 (a) Nitrogen sorption measurements and (b) DFT pore size distributions of the titania-shell CMS nanoparticles in comparison to the unmodified silica-CMS. A: CMS; B: 10Ti@CMS; C: 50Ti@CMS; D: 80Ti@CMS; E: 100Ti@CMS; F: 100Ti@CMS + TiNPs. For clarity reasons, the isotherms are shifted along the *y*-axis by 150 units each and the DFT pore size distributions are offset by 0.075 units.

The UV-Vis spectra of the titania-enriched shell CMS samples in Fig. 1a show an absorption band in the region of 220–240 nm. This absorption results from a ligand-to-metal charge transfer from oxygen to Ti(IV) as reported for titania incorporated in a silica network.[15,17] In particular, greater amounts of TEOT added to the reaction mixture result in a higher Ti-content of the samples and higher absorbance. In contrast, the pure silica nanoparticles (sample CMS, curve A) show negligible absorption in the measured UV-Vis range. These results suggest the incorporation of Ti atoms into the silica nanoparticles according to the Ti/Si ratio of the reactants.

Dynamic light scattering (DLS) curves (Fig. 1b) show that the dispersed particles have a nanoscopic size in all samples. We note that with increasing titania content in the external shell the CMS particle size is reduced. We attribute this behaviour to a more negative surface charge as the Ti-content in the shell increases (determined by ζ-potential measurements, see ESI†). This leads, on the one hand, to a higher repulsion and thus a lower tendency towards agglomeration, and, on the other hand, to different sizes of the solvation shells and the corresponding changes in hydrodynamic radius. Interestingly, the sample 100Ti@CMS + TiNPs shows a larger mean particle size than the sample 100Ti@CMS, which we attribute to the presence of the anatase nanocrystals on the titania-shell surface. It is likely that this size difference is caused not only by the dimensions of the titania nanocrystals, but also by the different surface charge and thus a different hydrodynamic radius in solution.

Nitrogen sorption measurements of all samples (Fig. 2a) exhibit the Type IV isotherms typical for mesoporous materials, with pore filling steps at around $p/p_0 = 0.3$–0.4. The isotherms of the titania-enriched shell samples show no significant changes with respect to the pure mesoporous silica nanoparticles (note that the isotherms are shifted along the *y*-axis for clarity), as well as BET surface areas and pore volumes, see Table 1, indicating

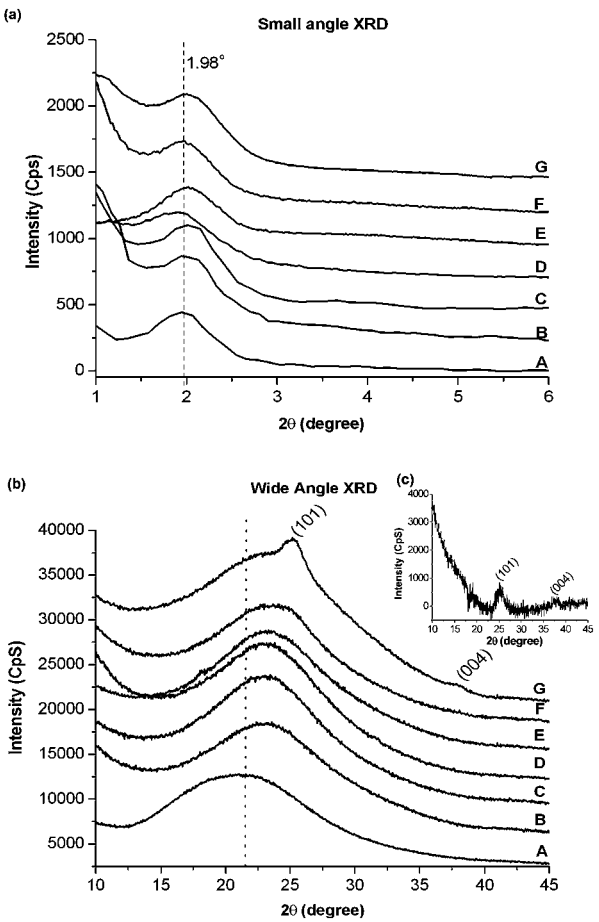

Fig. 3 (a) Small angle and (b) wide angle X-ray diffraction patterns of the titania-shell CMS nanoparticles; (c, inset) WAXS pattern of the sample 100Ti@CMS + TiNPs (F) after subtraction of the 100Ti@CMS pattern. A: CMS; B: 10Ti@CMS; C: 50Ti@CMS; D: 80Ti@CMS; E: 100Ti@CMS; F: 100Ti@CMS + TiNPs; G: 100Ti@CMS + TiNPs after calcination at 450 °C. For clarity reasons, the small angle XRD patterns are shifted along the *y*-axis by 100 units each (the pattern B by 400 units) and the wide angle XRD data are offset by 2500 units.

 This journal is © The Royal Society of Chemistry 2011

Downloaded by Ludwig Maximilians Universitaet Muenchen on 25/04/2013 13:29:51.
Published on 10 August 2011 on http://pubs.rsc.org | doi:10.1039/C0JM04528D

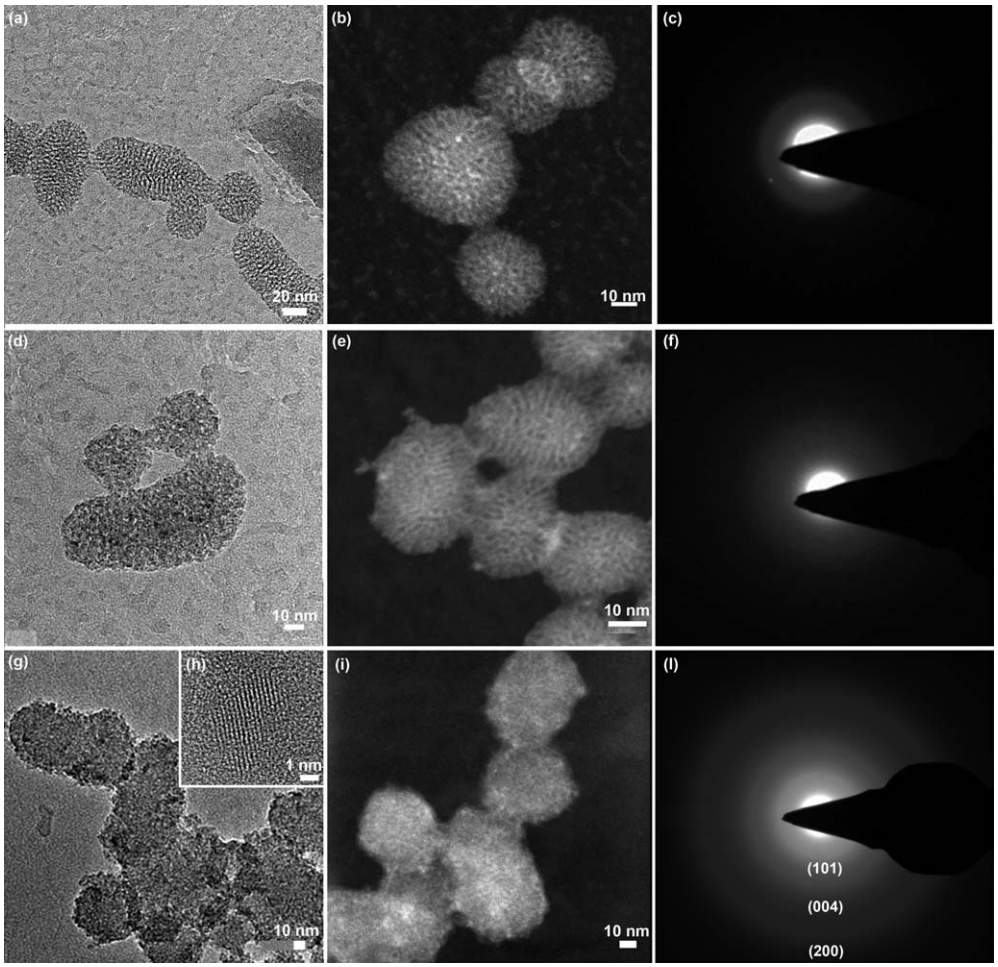

Fig. 4 Transmission electron micrographs (TEM, left column), scanning transmission electron micrographs (STEM, central column), and electron diffraction patterns (right column) of the samples (a–c) 10Ti@CMS; (d–f) 100Ti@CMS; (g–l) 100Ti@CMS + TiNPs. (h) represents the lattice fringes showing the crystallinity of the TiO_2 nanoparticles at the edge of the CMS nanoparticles depicted in micrograph (g).

that the titania inclusion in the silica shell does not affect the mesoporous features of the nanoparticles. All the particles show a pore size of around 3.7–3.8 nm, obtained by a DFT method, and uniform pore size distributions (Fig. 2b) except for 100Ti@CMS + TiNPs, having a slightly larger pore size of about 4.2 nm. Since the pore sizes of the *x*Ti@CMS samples do not decrease with respect to the pure CMS nanoparticles, we conclude that the addition of titania precursor leads to an enrichment of titanium dioxide species only at the outer shell of the mesoporous nanoparticles.

Small-angle X-ray scattering shows the first order (100)-like reflection at $2\theta = 1.98°$ for all titania-shell nanoparticles and the pure silica sample (Fig. 3a). The absence of higher order reflections indicates a worm-like mesoporous structure of the titania-shell CMS particles.

Wide-angle X-ray scattering (WAXS) for the CMS sample (Fig. 3b, trace A) shows the broad feature centered at 22° attributed to amorphous silica. This reflection shifts gradually to a higher angle (24°) as the titania content at the outer shell of the samples increases (traces from B to E). This behavior is attributed to the shorter Ti–O–Ti and Ti–O–Si bonds with respect to the Si–O–Si bonds.[26,27] The sample 100Ti@CMS + TiNPs (trace F) shows an additional shoulder in the WAXS pattern at about 25° that is attributed to the (101) reflection of anatase (see also Fig. 3c, in which the contribution of the amorphous part is subtracted). The anatase crystallite size estimated with the Debye–Scherrer equation is about 5 nm, in line with the previously reported results.[19,22] This becomes more evident upon additional calcination of sample 100Ti@CMS + TiNPs at 450 °C (Fig. 3b, trace G), showing the (101) and (004) reflections of the crystalline anatase phase. The retention of the worm-like mesoporous structure upon calcination was also assessed by SAXS (Fig. 3a, trace G). However, after such thermal treatment the dried particles are no longer colloidally dispersible.

The presence of anatase nanocrystalline clusters in sample 100Ti@CMS + TiNPs even without calcination is observed with transmission electron microscopy (HRTEM, Fig. 4g). In this micrograph dark spots, resulting from the higher contrast due to Ti compared to Si, are clearly observed at the edge of the CMS nanoparticles (in grey). Correspondingly, scanning transmission electron microscopy (STEM, Fig. 4i) shows a brighter region attributed to Ti oxide at the CMS surface. Electron diffraction patterns (Fig. 4l) and a high-resolution TEM image (HRTEM, Fig. 4h) clearly show nanocrystalline

Downloaded by Ludwig Maximilians Universitaet Muenchen on 25/04/2013 13:29:51.
Published on 10 August 2011 on http://pubs.rsc.org | doi:10.1039/C0JM04528D

Table 2 Relative ratio of titanium to silicon obtained by EDS and elemental analysis (ICP) on different *x*-titania-shell CMS nanoparticles and the reference pure silica nanoparticles

Sample	Ti/Si (from EDS)	Ti/Si (from ICP)
CMS	—	—
10Ti@CMS	0.020	0.009
100Ti@CMS	0.031	0.016
100Ti@CMS + TiNPs	0.199	0.134

clusters, assigned to the anatase phase, at the outer surface of the CMS nanoparticles.

TEM images of the other colloidal 10Ti@CMS and 100Ti@CMS nanoparticles (Fig. 4a and d, respectively) show monodispersed, highly porous particles with worm-like mesoporous structure. The presence of the titania-enriched shell is almost negligible for the 10Ti@CMS sample (Fig. 4a and b), whereas for sample 100Ti@CMS it is indicated by dark spots in the TEM image (Fig. 4d) and bright clusters in STEM mode (Fig. 4e). We conclude that the incidence of such contrast variations due to titanium enrichment increases as the amount of titania-precursors in the synthesis increases. Moreover, as already observed in the WAXS measurements, the electron diffraction patterns of samples 10Ti@CMS and 100Ti@CMS (Fig. 4c and f, respectively) show only amorphous phases.

The results of Energy Dispersive Spectroscopy (EDS) and elemental analysis (ICP) shown in Table 2 demonstrate that the Ti/Si ratio in the nanoparticles is significantly lower than the molar ratios of TEOT/TEOS precursors in the particle synthesis.

This indicates that the incorporation of titania into the shell of the mesoporous nanoparticles is kinetically limited and that some of the TEOT is hydrolyzed and polymerized not only on the particle surface but also in solution, forming soluble species which are removed during the washing step. The formation of anatase nanocrystals strongly increases the fraction of Ti obtained on the sample 100Ti@CMS + TiNPs.

N3-Dye measurements

The results discussed above clearly indicate that an amorphous titania phase is formed through the delayed co-condensation approach on the mesoporous silica core. Moreover, the titania-enriched shell is able to serve as preferential nucleation site for the nanocrystalline anatase clusters. In this way, the sol–gel approach leads to fully inorganic silica-core titania/silica-shell mesoporous nanoparticles, which can exhibit an orthogonal chemical functionality, *i.e.* a spatially resolved affinity to different chemical species.

As a proof of principle we have examined the adsorption of a ruthenium-centered polypyridyl dye, N3. This complex possesses four carboxyl groups and is expected to preferentially bind to the titania-phase of the nanoparticles.[18] Specifically, we examined both 100Ti@CMS samples, with and without the anatase nanocrystallites, and compared the results to the pure silica CMS nanoparticles. The N3-dye solutions were measured by UV-Vis spectroscopy before and after the uptake into the *x*Ti@CMS and CMS samples (Fig. 5a).

After the adsorption step, the UV-Vis spectra of the solutions show the remaining amount of the dye that is not adsorbed into the samples. The N3-solution after the uptake into the 100Ti@CMS + TiNps shows the lowest absorbance (solid line), whereas the dye solution of the reference CMS nanoparticles

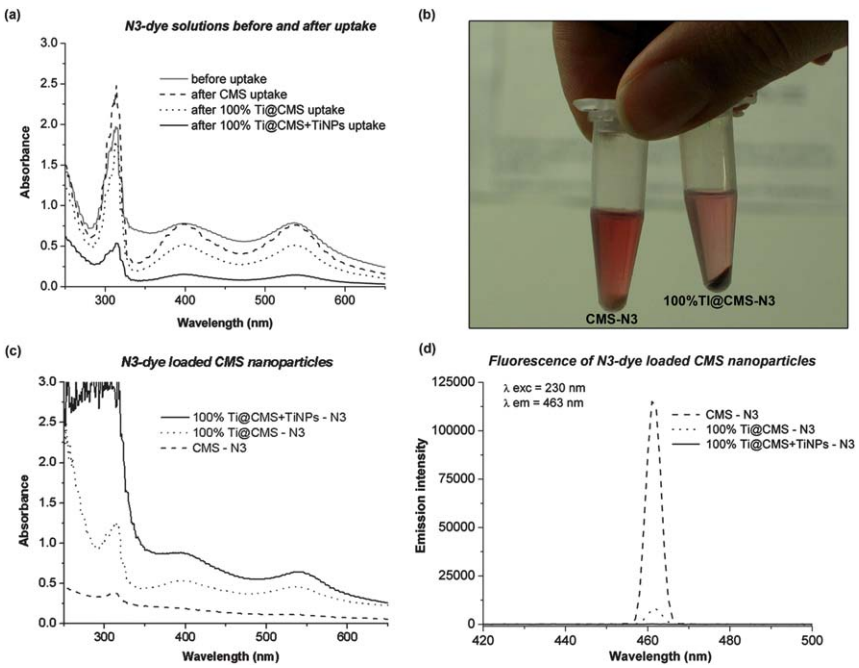

Fig. 5 N3-Dye adsorption experiments on the samples: CMS (dashed line), 100%Ti@CMS (dotted line) and 100%Ti@CMS + TiNPs (solid line). (a) UV-Vis absorption spectra of the N3 solutions before (solid line in grey) and after uptake in different sample solutions; (b) photograph of the reference sample CMS and of the 100%Ti@CMS after N3 uptake with the supernatant solution analyzed in (a). (c) UV-Vis adsorption spectra of the nanoparticles as colloidal solution in water after N3-dye adsorption; (d) fluorescence spectra of the same colloidal nanoparticle solution, clearly showing the emission quenching of the N3 adsorbed on the sample 100%Ti@CMS + TiNPs.

 This journal is © The Royal Society of Chemistry 2011

Downloaded by Ludwig Maximilians Universitaet Muenchen on 25/04/2013 13:29:51.
Published on 10 August 2011 on http://pubs.rsc.org | doi:10.1039/C0JM04528D

shows the highest absorbance (dashed line) in comparison to the initial N3-solution before the uptake (grey line). The colloidal suspensions of the N3-loaded nanoparticles were washed and centrifuged several times in order to desorb any physisorbed N3-dye and were then measured again by UV-Vis spectroscopy (Fig. 5c). The highest adsorption levels are obtained for the 100Ti-containing shell CMS nanoparticles with the anatase nanocrystallites (100Ti@CMS + TiNps, solid line), whereas the lowest dye loadings were recorded for the reference CMS nanoparticles (dashed line). These results are also clearly visible in the photograph in Fig. 5b, showing the nanoparticles after the centrifugation at the end of the dye-adsorption step. The sample 100Ti@CMS has attained a darker color than the CMS sample, leaving the supernatant solution less colored with respect to that of the reference CMS sample. In conclusion, UV-Vis spectroscopy indicates a strong interaction of the N3-dye with the surface titania-phase of the CMS nanoparticles. Despite the high porosity of the mesoporous silica core, the pure CMS particles do not reach the same adsorption values as the samples with the titania-shell. This affinity between the N3-molecules and the titania-phase is increased when anatase nanocrystallites are attached to the titania-shell on the particles' surface.

To further elucidate the localization of the N3-molecules on the titania part of the core–shell nanoparticles, the fluorescence emission of the N3-loaded nanoparticles was recorded (Fig. 5d). It is known that the strong bond between the titania surface and the ruthenium complex enables the titania to quantitatively quench the fluorescence emission of the dye.[28] Strikingly, no fluorescence was detected for the N3-loaded 100Ti@CMS + TiNPs sample, and only a weak emission at 463 nm was recorded for the 100Ti@CMS, without the anatase nanocrystallites. In contrast, the reference CMS sample, showing very low levels of dye adsorption, exhibits a very intense fluorescence emission. These results show that the N3-dye molecules are selectively adsorbed at the titania shell on the CMS nanoparticles and not into the highly porous silica mesostructure of the core. In particular, the presence of anatase nanocrystallites at the titania-enriched shell of CMS nanoparticles leads to the highest dye adsorption values and the best selectivity for dye adsorption, as demonstrated by the complete quenching of its fluorescence emission.

Conclusions

We report on the synthesis of fully inorganic colloidal mesoporous nanoparticles with a silica-core and a titania/silica-shell. In order to obtain the selective inclusion of titania into the outer shell of mesoporous silica nanoparticles, a delayed co-condensation method using TEOT as titania precursor was applied. By varying the amount of TEOT added in the synthetic step, we show enrichment of an amorphous titania phase in the outer-shell at the particles' surface. After template extraction, the CMS nanoparticles containing the highest amount of Ti in the shell (100Ti@CMS sample) were used to nucleate titania nanocrystallites from a $TiCl_4$ solution in benzyl alcohol at 60 °C. The presence of nanocrystalline anatase clusters could be observed on the surface of the colloidal 100Ti@CMS + TiNPs nanoparticles by HRTEM and STEM.

All titania-enriched shell CMS nanoparticles show a wormlike mesoporous structure, high surface area and pore volume, and a nanoscopic particle size similar to pure silica CMS nanoparticles.

To examine the orthogonal functionality of these fully inorganic silica-core titania-shell mesoporous nanoparticles, the adsorption and retention of a ruthenium-centered polypyridyl dye (N3) were investigated. UV-Vis and fluorescence spectroscopy indicate a strong interaction of the N3-dye only with the titania-phase at the outer shell of the CMS nanoparticles, thus demonstrating the selective adsorption of N3-molecules on the titania-phase and not into the highly porous silica core. We envision the use of such multiple core–shell inorganic nanoparticles in applications such as targeted drug delivery where colloidal stability and orthogonal functionality of both oxides are desired. Generalizing, this could also include access to different all-inorganic core–shell mesoporous nanoparticles offering orthogonal functionalities with the benefit of much higher thermal and chemical stability, as well as novel functionalities (catalytic, optical, magnetic, *etc*.) not accessible with organic moieties.

Acknowledgements

Support from DFG-SFB 486 and 749 and from the NIM Cluster (LMU München) is gratefully acknowledged.

References

1 J. Kobler and T. Bein, *ACS Nano*, 2008, **11**, 2324–2330.
2 A. Schlossbauer, J. Kecht and T. Bein, *Angew. Chem., Int. Ed.*, 2009, **48**, 3092–3095.
3 V. Cauda, C. Argyo, A. Schlossbauer and T. Bein, *J. Mater. Chem.*, 2010, **20**, 4305–4311.
4 J. Kobler, K. Möller and T. Bein, *ACS Nano*, 2008, **2**, 791–799.
5 V. Cauda, A. Schlossbauer, J. Kecht, A. Zürner and T. Bein, *J. Am. Chem. Soc.*, 2009, **131**, 11361–11370.
6 J. Kecht, A. Schlossbauer and T. Bein, *Chem. Mater.*, 2008, **20**, 7207–7214.
7 M. C. Lechmann, D. Kessler and J. S. Gutmann, *Langmuir*, 2009, **25**, 10202–10208.
8 M. H. Bartl, S. W. Boettcher, K. L. Frindell and G. D. Stucky, *Acc. Chem. Res.*, 2005, **38**, 263–271.
9 M. K. Nazeeruddin, A. Kay, I. Rodicio, R. Humpbry-Baker, E. Müller, P. Liska, N. Vlachopoulos and M. Graetzel, *J. Am. Chem. Soc.*, 1993, **115**, 6382–6390.
10 J. W. Lee, M. R. Othman, Y. Eom, T. G. Lee, W. S. Kim and J. Kim, *Microporous Mesoporous Mater.*, 2008, **116**, 561–568.
11 D.-W. Lee, S.-K. Ihm and K.-H. Lee, *Chem. Mater.*, 2005, **17**, 4461–4467.
12 W. K. Oh, S. Kim, M. Choi, C. Kim, Y. S. Jeong, B.-R. Cho, J.-S. Hahn and J. Jang, *ACS Nano*, 2010, **4**, 5301–5313.
13 R. Abe, K. Hara, K. Sayama, K. Domen and H. Arakawa, *J. Photochem. Photobiol., A*, 2000, **137**, 63–69.
14 Q. Li, Z. Jin, Z. Peng, Y. Li, S. Li and G. Lu, *J. Phys. Chem. C*, 2007, **111**, 8237–8241.
15 G. A. Eimer, S. G. Casuscelli, G. E. Ghione, M. E. Crivello and E. R. Herrero, *Appl. Catal., A*, 2006, **298**, 232–242.
16 J. Kobler, B. V. Lotsch, G. A. Ozin and T. Bein, *ACS Nano*, 2009, **3**, 1669–1676.
17 Y. Li and S.-J. Kim, *J. Phys. Chem. B*, 2005, **109**, 12309–12315.
18 T. Fernandez, U. K. Samersen, X. Joseph and N. V. J. Unnikrishnan, *J. Mater. Process. Technol.*, 2008, **202**, 528–535.
19 D. Fattakhova-Rohlfing, J. M. Szeifert, Q. Yu, V. Kalousek, J. Rathousky and T. Bein, *Chem. Mater.*, 2009, **21**, 2410–2417.
20 D. R. Sahu, L. Y. Hong, S.-C. Wang and J.-L. Huang, *Microporous Mesoporous Mater.*, 2009, **117**, 640–649.

View Article Online

21 L. Zhao, J. Yu and B. Cheng, *J. Solid State Chem.*, 2005, **178**, 1818–1824.
22 J. M. Szeifert, J. M. Feckl, D. Fattakhova-Rohlfing, Y. Liu, V. Kalousek, J. Rathousky and T. Bein, *J. Am. Chem. Soc.*, 2010, **132**, 12605–12611.
23 G. Garnweitner, M. Antonietti and M. Niederberger, *Chem. Commun.*, 2005, 397–399.
24 M. Grätzel, *Acc. Chem. Res.*, 2009, **42**, 1788–1789.
25 A. Hagfeldt and M. Grätzel, *Acc. Chem. Res.*, 2000, **33**, 269–277.
26 X. Orignac, H. C. Vasconcelos and R. M. Almeida, *J. Non-Cryst. Solids*, 1997, **217**, 155–161.
27 W. Dong, Y. Sun, C. W. Lee, W. Hua, X. Lu, Y. Shi, S. Zhang, J. Chen and D. Zhao, *J. Am. Chem. Soc.*, 2007, **129**, 13894–13904.
28 D. Pan, N. Klymyshyn, D. Hu and H. P. Lu, *Appl. Phys. Lett.*, 2006, **88**, 093121.

Downloaded by Ludwig Maximilians Universitaet Muenchen on 25/04/2013 13:29:51.
Published on 10 August 2011 on http://pubs.rsc.org | doi:10.1039/C0JM04528D

 This journal is © The Royal Society of Chemistry 2011